Plant and Cell Physiology Advance Access published April 15, 2016

**Title;**

Jasmonate-responsive ERF transcription factors regulate steroidal glycoalkaloid biosynthesis in tomato.

**Running title;**

Regulation of SGA biosynthesis in tomato

**Corresponding author;**

Name; Tsubasa Shoji

Affiliation; Graduate School of Biological Sciences, Nara Institute of Science and Technology

Address; Takayama 8916-5, Ikoma, Nara 630-0101, Japan

Telephone; +81-743-72-5521

Fax; +81-743-72-5529

E-mail: t-shouji@bs.naist.jp

**Subject areas;**

(3) regulation of gene expression, (9) natural products.

**Number of black and white figures, color figures, tables and type and number of**

**supplementary material;**

Black and white figures; 4

Color figures; 3

Tables; 0

Supplementary figures; 5

Supplementary tables; 10

**Title and running head;**

Title; Jasmonate-responsive ERF transcription factors regulate steroidal glycoalkaloid biosynthesis in tomato.

Running head; Regulation of SGA biosynthesis in tomato



**Authors**

Chonprakun Thagun[1], Shunsuke Imanishi[2], Toru Kudo[3], Ryo Nakabayashi[4], Kiyoshi Ohyama[5], Tetsuya Mori[4], Koichi Kawamoto[6], Yukino Nakamura[3], Minami Katayama[3], Satoko Nonaka[6], Chiaki Matsukura[6], Kentaro Yano[3], Hiroshi Ezura[6], Kazuki Saito[4,7], Takashi Hashimoto[1], and Tsubasa Shoji[1]

**Authors' addresses;**

[1]Graduate School of Biological Sciences, Nara Institute of Science and Technology, Ikoma, 630-0101, Japan

[2]Institute of Vegetable and Tea Science, National Agriculture and Food Research Organization, Tsu, 514-2392, Japan

[3]Department of Life Sciences, School of Agriculture, Meiji University, Kawasaki, 214-8571, Japan

[4]RIKEN Center for Sustainable Resource Science, Yokohama, 230-0045, Japan

[5]Department of Chemistry and Materials Science, Tokyo Institute of Technology, Meguro-ku, 152-8551, Japan

[6]Graduate School of life and Environmental Sciences, University of Tsukuba, Tsukuba, 305-8577, Japan

[7]Graduate School of Pharmaceutical Sciences, Chiba University, Chiba, 260-8675, Japan



**Abbreviations;**

ACAA, acetyl-CoA *C*-acetyltransferase; bHLH, basic helix-loop-helix; CaMV, cauliflower mosaic virus; DMPP, dimethylallyl pyrophosphate; D14SR, Δ14-sterol reductase; DWF5, sterol reductase; DWF7, sterol C-5 desaturase; EAR, ERF-associated amphiphilic repression; EMSA, electrophoretic mobility shift assay; ERF, ethylene response factor; GAME, glycoalkaloid metabolism; GC-MS, gas chromatography-mass spectrometry; GFP, green fluorescent protein; GUS, β-glucuronidase; HMGS, hydroxymethylglutaryl-CoA synthase; HMGR, 3-hydroxy-3-methylglutaryl CoA reductase; HYD1, 3β-hydroxysteroid-Δ8Δ7-isomerase; IDI, isopentenyl-diphosphate Δ-isomerase; IPP, isopentenyl pyrophosphate; JA, jasmonate; JAZ, jasmonate ZIM-domain protein; JRE, jasmonate-responsive ERF; LC-QTOF-MS, liquid chromatography-quadrupole

time-of-flight-mass spectrometry; MeJA, methyl jasmonate; O14DM, obtsuifoliol 14α-demethylase; ORCA3, octadecanoid-derivative responsive *Catharanthus* 3; qRT-PCR, quantitative reverse transcription-PCR; SCDH, sterol-4α-carboxylate 3-dehydrogenase; SGA, steroidal glycoalkaloid; SMO2, sterol 4α-methyl oxidase 2; SQO, squalene monooxygenase; SSR2, sterol side chain reductase 2.

**Footnotes;**

None

**Abstract**

Steroidal glycoalkaloids (SGAs) are cholesterol-derived specialized metabolites produced in species of the Solanaceae. Here, we report that a group of jasmonate-responsive transcription factors of the ETHYLENE RESPONSE FACTOR family (JREs), are close homologs of alkaloid regulators in *Cathranthus roseus* and tobacco and regulate production of SGAs in tomato. In transgenic tomato, overexpression and dominant suppression of *JRE*s caused drastic changes in SGA accumulation and in the expression of genes for metabolic enzymes involved in the multistep pathway leading to SGA biosynthesis, including the upstream mevalonate pathway. Transactivation and DNA-protein binding assays demonstrate that JRE4 activates the transcription of SGA biosynthetic genes by binding to GCC box-like elements in their promoters. These JRE-binding elements occur at significantly higher frequencies in proximal promoter regions of the genes regulated by *JRE*s, supporting the conclusion that JREs mediate transcriptional coordination of a series of metabolic genes involved in SGA biosynthesis.

**Keywords**

jasmonates, steroidal glycoalkaloids, tomato, transcription factors

## Text

### *Introduction*

Plants have evolved multitudes of defense and adaptation mechanisms to survive in fluctuating environments. To ward off threats imposed by pathogens and pests, plants produce and accumulate toxic substances, including a diverse array of alkaloids, terpenoids, and other metabolites with bioactive properties (Bednarek and Osbourn 2009). Although these plant-derived chemicals, or phytochemicals, are widely exploited by humans as valuable compounds, they are often unwanted in food crops because of adverse impacts on human health (Betz 1999). Accordingly, elimination or reduction of such phytochemicals is a critical aim in plant breeding. Complex metabolic pathways, encompassing precursor-supplying primary pathways and downstream specialized pathways, produce defense compounds. Tight regulation, often involving transcriptional coordination of structural genes, is required to ensure restrained implementation of these costly chemical defenses, which often impose burdens on growth and development in plants (Baldwin 1998).

Jasmonates (JAs) play central signaling roles in a wide range of plant resistance and developmental responses (Wasternack and Hause 2013), including the elicitations of defense chemical pathways. Indeed, methyl jasmonate (MeJA) has been widely used as an elicitor to induce the production of secondary metabolites in plant culture (Yukimune et al. 1996). Perception of JA signals and the subsequent signal transduction pathway steps, mediated by

CORONATINE INSENSITIVE 1, JASMONATE ZIM-DOMAIN proteins (JAZs) and JAZ-interacting transcription factors, have been elucidated through molecular and genetic studies and are conserved among plant species (Wasternack and Hause 2013). However, less is known about the molecular mechanisms linking JA signaling with downstream defense-related metabolism (De Geyter et al. 2012). A group of JA-inducible ETHYLENE RESPONSE FACTOR (ERF) transcription factors, categorized into clade 2 of group IXa (Nakano et al. 2006, Shoji et al. 2010, Shoji et al. 2013) have been found to play regulatory roles in JA-induced alkaloid biosynthesis in distinct species. For instance, OCTADECANOID-DERIVATIVE RESPONSIVE CATHARANTHUS 3 (ORCA3) controls the JA-dependent production of monoterpenoid indole alkaloids, including clinically important compounds, in the medicinal species *Catharanthus roseus* (van der Fits and Memelink 2000). Similarly, the JA-induced formation of ornithine-derived nicotine is regulated by ERF189 in tobacco (Shoji et al. 2010). Both *ORCA3* and *ERF189* mediate the coordinated transcription of a series of metabolic and transport genes (Shoji et al. 2009) involved in the alkaloid pathways by recognizing specific GCC box-like elements found in promoters of the target genes (van der Fits and Memelink 2001, Shoji et al. 2010, Shoji and Hashomoto 2011a). The JA-inducible expression of *ORCA3* and *ERF189* is regulated by a homologs of the basic helix-loop-helix (bHLH)-family MYC2 transcription factor (Zhang et al. 2011, Shoji and Hashimoto 2011b). MYC2 is a JAZ-interacting factor, involved in the

regulation of a wide range of downstream JA responses (Kazan and Manners 2013).

Steroidal glycoalkaloids (SGAs), which occur in certain species of Solanaceae and Lilaceae families, are nitrogen-containing compounds with a glycosylated steroidal backbone derived from cholesterol. Based on their cytotoxic properties, SGAs have been proposed to function in plant defense against biotic threats (Friedman 2002, Friedman 2006). SGAs are present as toxic and anti-nutritional compounds in inedible parts of solanaceous vegetables, such as immature green fruits of tomato and sprouts and green peels of potato tubers (Friedman 2002, Friedman 2006, Iijima et al. 2013). In tomato, α-tomatine, derived from its aglycone tomatidine through elaborate glycosylation steps, is the predominant SGA in green organs, while its less toxic derivatives are found in red ripe fruits (Iijima et al. 2009). After early molecular studies on glycosyltransferases involved in the glycosylation (Moehs et al. 1997, Itkin et al. 2011), a series of *GLYCOALKALOID METABOLISM* (*GAME*) genes were identified as responsible for enzymatic steps from cholesterol to SGAs in tomato and potato (Itkin et al. 2013). STEROL SIDE CHAIN REDUCTASE 2 (SSR2) plays a key role diverting the metabolic flow to cholesterol formation from cycloartenol (Sawai et al 2014). Similar to other metabolic genes that form clusters in plant genomes (Boycheva et al. 2014), *GAME* genes are clustered in both the tomato and potato genomes (Itkin et al. 2013).

Cárdenas et al. (2016) recently identified five tomato *ERF* genes phylogenetically related to alkaloid-regulating *ORCA3* and *ERF189*, and reported that one of them regulates

the metabolic genes involved in the biosynthesis of SGAs in tomato and potato (Cárdenas et al. 2016). Here, we report characterization of these genes, which we term *Jasmonate-Responsive ERF* (*JRE*) genes, as well as of a sixth related *JRE* in tomato. We performed transcript profiling and metabolite analyses of transgenic tomato lines with altered *JRE* function. We demonstrated that *JRE*s play central roles in the transcriptional regulation of pathways leading to SGA formation, from the isoprenoid-supplying mevalonate pathway to GAME-mediated steps after cholesterol. Transactivation and DNA-protein binding studies indicated that JRE4 positively controls the biosynthesis genes by recognizing GCC box-like elements in their promoters. Significant enrichment of putative JRE-binding elements in proximal 5'-flanking regions of *JRE*-regulated genes, including those involved in SGA biosynthesis, further support the conclusion of *JRE*-mediated transcriptional coordination of these genes.

## *Results*

### Six *JRE* genes and their expression patterns in tomato

In tomato, there is a gene cluster (spanning about 100 kb) with five clade 2 *ERF* genes of group IXa on chromosome I (Cárdenas et al. 2016); we found that one additional *ERF* gene of this clade resides as a singleton on chromosome V (**Fig. 1a**). Since all six *ERF* genes were inducible by jasmonate (see below), we named them *Jasmonate-Responsive ERF* (*JRE*) *1*

(Solyc01g090300), *JRE2* (Solyc01g090310), *JRE3* (Solyc01g090320), *JRE4* (Solyc01g090340) *JRE5* (Solyc01g090370) and *JRE6* (Solyc05g050790). Note that *JRE1*, *JRE2*, *JRE3*, *JRE4*, and *JRE5* respectively correspond to *GAME9-like1*, *GAME9-like2*, *GAME9-like3*, *GAME9*, and *GAME9-like4* reported in a very recent study (Cárdenas et al. 2016).

Based on alignment of amino acid sequences of the conserved DNA-binding domain, a phylogenetic tree including JREs from tomato and related ERF proteins from Arabidopsis, *Catharanthus roseu*s, and tobacco was generated to examine the evolutionary relationships among the members (**Fig. 1b**). As defined previously (Shoji et al. 2013), clade 2 is divided into 4 subgroups. JRE3 and JRE4 were placed in clade 2-2b, and the remaining four JREs were in clade 2-3 (**Fig. 1b**).

We examined the expression patterns of *JRE* genes along with SGA biosynthetic *3-hydroxy-3-methylglutaryl CoA reductase* (*HMGR1*), *sterol 4α-methyl oxidase 2* (*SMO2*), and *GAME1* genes in tomato tissues using quantitative Reverse Transcription (qRT)-PCR (**Fig. 2** and numerical values in **Supplementary Table S1**). Both *JRE* genes and SGA biosynthesis genes were expressed in organs from 7-week-old plants and no apparent organ specificity was observed (**Fig. 2a**). *JRE4* was the most highly expressed *JRE* in nearly all examined tissues, though in roots and fruits at certain stages, the predominance of *JRE4* was diminished, mainly due to decreased *JRE4* expression in the tissues. The levels of toxic

SGAs, such as α-tomatine, as well as their production drastically decrease during fruit ripening in parallel with increased catabolism of toxic SGAs to less toxic forms (Iijima et al. 2009). In accordance with such changes, expression of SGA biosynthesis genes and some members of *JRE*s, *JRE1*, *JRE2*, and *JRE4*, progressively decreased as fruits matured (**Fig. 2b**). Except for *HMGR1*, expression of which declined clearly at the breaker stage, decreases in the SGA biosynthesis and *JRE* gene expression were most evident during green fruit stages (**Fig. 2b**), when fruits were rapidly enlarging, rather than during later color-changing stages. Expression levels of *JRE*s in cultured hairy roots were comparable to or somewhat higher than those in tissues from greenhouse-grown plants, suggesting the usefulness of the cultured material in studies on *JRE*s and SGA biosynthesis. MeJA coordinately induced SGA biosynthesis genes in tomato hairy roots (**Fig. 2c**). All *JRE*s were induced by MeJA treatment in tomato hairy roots, but the induction kinetics in terms of magnitude and timing varied among the members (**Fig. 2c**). *JRE4* and *JRE6* were gradually induced during the 24-h duration. Acute and strong induction within 30 min followed by a sharp decline was characteristic of *JRE1*, *JRE2*, and *JRE3*. Induction of *JRE5* peaked at 4 h after the start of the treatment.

**Generation of transgenic tomato lines with altered function of *JRE* genes**

To study effect of altered *JRE* function on gene expression and metabolism in tomato, stable

transgenic tomato lines of plants and hairy roots were generated by *Agrobacterium*-mediated transformation. Two *JRE4* overexpression (*JRE4-OX*) lines of plants (lines OX1 and OX12) were established by introducing *JRE4* cDNA under the control of cauliflower mosaic virus (CaMV) 35S promoter. *JRE4* was chosen as a target gene for overexpression because it is the main *JRE* expressed in tomato tissues (**Fig. 2**). In leaves of the *JRE4-OX* lines, high expression of *JRE4* transcript was confirmed; this expression did not significantly change with MeJA treatment (**Supplementary Fig. S1a**). By contrast, MeJA induced the endogenous *JRE4* gene in wild-type controls (**Supplementary Fig. S1a**). No visible abnormalities were observed in the *JRE4*-OX plants (**Supplementary Fig. S1b**).

We chose a dominant suppression strategy to compromise *JRE* function, since the closely related *JRE* genes could have overlapping functions. For this purpose, JRE3, JRE4, and JRE5 were fused at their C termini with the ERF-associated amphiphilic repression (EAR) motif, which dominantly suppresses expression of genes targeted by transcription factors (Hiratsu et al. 2003). The *JRE-EAR*s were overexpressed using the CaMV35S promoter in transgenic tomato hairy roots; two independent lines (lines #1 and #2) for each construct were selected and analyzed. Overexpression of the introduced *JRE* genes was confirmed in *JRE-EAR* lines using qRT-PCR (**Supplementary Fig. S2**). Consistent with different expression levels of the endogenous *JRE* genes (**Fig. 2**), the degrees of overexpression relative to vector controls varied among the lines with different fusion

constructs. There was significant reduction of off-target *JRE* gene expression (e. g. *JRE1* and *JRE2* in all *JRE-EAR* lines, *JRE6* in *JRE3-EAR* and *JRE5-EAR* lines) (**Supplementary Fig. S2**), suggesting down-regulation of the *JRE*s by the *JRE-EAR* fusions. There were slight variations of growth and morphology among the lines (not shown), but they were within the range normally observed for hairy root cultures.

**Transcript profiling in overexpression and dominant-suppression lines of *JRE*s**

To clarify the regulatory function of JRE transcription factors in tomato, we investigated the effects of altered *JRE* function on the transcriptome to reveal genes targeted by *JRE*s. Comparative transcript profiling was carried out using the overexpression and dominant-suppression transgenic lines with a custom tomato oligoarray representing over 40,000 transcripts (Ruiu et al. 2015). Total RNA from each line was labelled and hybridized to the array. As control samples for comparison, wild-type plants for overexpression and empty-vector control lines for suppression were included. To examine the profiles in distinct types of tissues as well as after JA elicitation, leaves of *JRE4-OX* lines and hairy roots of suppression lines treated with MeJA were used for analysis.

Array oligos representing genes up-regulated in *JRE4-OX* lines and down-regulated in *JRE-EAR* lines are listed in **Supplementary Table S2** and **Table S3**, respectively; the list of the genes represented is in **Supplementary Table S4**. A large number metabolic genes

involved in SGA biosynthesis were among the *JRE*-regulated genes; 24 genes regulated in either *JRE4-OX* or *JRE-EAR* lines (**Fig. 3** and **Supplementary Table S5**). All genes, except two (Solyc05g055760 for *IDI* and Solyc02g069490 for *SSR2*), whether they satisfied both listing criteria ($R_{ox}$>5.0, Q<0.85) or not, showed trends of signal increases in *JRE4-OX* lines as well as decreases in *JRE-EAR* lines. The *JRE*-regulated metabolic genes were involved in nearly all branches of the pathway leading to SGAs from the upstream mevalonate pathway to cholesterol biosynthesis and downstream aglycone formation and glycosylation (**Fig. 3**). The extent of regulation generally seemed greater for later steps, especially those after cholesterol (**Fig. 3**); *GAME* genes were especially responsive to alterations of *JRE* function (**Supplementary Table S2** and **Table S3**). All of the biosynthesis genes were similarly suppressed by *JRE3-EAR*, *JRE4-EAR*, and *JRE5-EAR*; this tendency was corroborated by the unbiased distribution of probes for SGA biosynthesis genes (**Supplementary Fig. S3**).

To validate the results of microarray analyses, transcript levels of SGA biosynthesis genes were analyzed in *JRE4-OX* and *JRE4-EAR* lines by qRT-PCR. Increased expression of the genes, except *acetyl-CoA C-acetyltransferase* (*ACAA*), was observed in leaves of *JRE4-OX* lines relative to wild-type controls in both MeJA-treated and mock-treated conditions (**Fig. 4a**). Consistent with the microarray analysis results, the degree of up-regulation in *JRE4-OX* lines was greater for genes involved in later parts of the pathway (**Fig. 4a**). We also found clear up-regulation of *SMO1* and *GAME1* but not *HMGR1* of the

mevalonate pathway in roots from *JRE4-OX* plants (**Supplementary Fig. S4**). In transgenic hairy roots expressing *JRE4-EAR*, all of the examined SGA biosynthesis genes were suppressed to 28 to 70% levels relative to the controls (**Fig. 4b**).

**Metabolic impact of altered *JRE4* function**

To clarify how altered *JRE4* function affects SGA-related metabolism in tomato, we examined metabolite levels in leaves from *JRE4-OX* plants exposed to MeJA vapor (**Fig. 5a**) and hairy roots of a *JRE4-EAR* line treated with MeJA (**Fig. 5b**). SGAs, including the predominant α-tomatine, were extracted and measured using liquid chromatography-quadrupole time-of-flight-mass spectrometry (LC-QTOF-MS), whereas more hydrophilic substances, including pathway intermediates and other sterols and triperpenoids, were analyzed using gas chromatography-mass spectrometry (GC-MS). In the *JRE4-OX* line (line OX1), the level of α-tomatine increased 2.1-fold relative to wild-type controls, while in the *JRE4-EAR* line (line #1), clear reductions of α-tomatine to 47 % level of controls were observed. Similar changes were observed for other SGAs (**Supplementary Table S6**, **Supplementary Figure S5**). Cholesterol, a sterol precursor of SGAs, increased 1.5-fold in the *JRE4-EAR* line. The phytosterols campesterol and stigmasterol did not show any significant changes except for a 32 % decrease of stigmasterol in the *JRE4-OX* line (**Fig. 5**). Cycloartenol and lanosterol, the first tetracyclic triperpenoid intermediates, were

markedly decreased in the *JRE4-OX* line, to 9 and 15 % of levels in the control, respectively, while a 3.3-fold increase of cycloartenol and a 2.9-fold increase of lanosterol were observed in the *JRE4-EAR* line. Triterpenoids, namely α-amyrin, β-amyrin, and lupeol, were increased 1.3- to 1.5-fold in the *JRE4-OX* line and decreased to 14 to 80 % of the control levels in the *JRE4-EAR* line. Squalene decreased to 48 % of that in the control in the *JRE4-OX* line and did not significantly change in the *JRE4-EAR* line.

**JRE4 activates transcription of SGA biosynthesis genes by binding to GCC box-like promoter elements**

To examine whether JRE4 activates the transcription of SGA biosynthesis genes *in vivo* through their 5'-flanking regions, transient transactivation assays were performed in tomato fruits using *Agrobacterium*-mediated infection, or agroinjection, for gene delivery. For transient expression, the *β-glucuronidase* (*GUS*) reporter was placed downstream of the 5'-flanking region of *sterol reductase* (*DWF5*) (-1500 to -1; counted from the first ATG) or *GAME4* (-1500 to -1) (**Fig. 6a**). The individual reporter constructs and a CaMV 35S promoter-driven *JRE4* effector were co-delivered into tomato fruits by agroinjection along with a CaMV 35S promoter-driven *green fluorescent protein* (*GFP*) reference construct. The expression levels of the *GUS* reporter genes were analyzed by qRT-PCR and normalized to that of the reference *GFP* gene (**Fig. 6b**). *DWF5* and *GAME4* promoter-driven *GUS*

reporter genes were up-regulated 3.8- and 8.2-fold by *JRE4* overexpression, respectively, indicating that the *JRE4*-mediated gene activation was dependent on regions included in the reporter constructs. The 1,500-bp region of *DWF5* could be trimmed to a relatively short span (-285 to -1) without losing reporter responsiveness (10.6-fold) (**Fig. 6b**) and basal activity, indicating the functional importance of this proximal region.

JRE4 recognizes two structurally related elements, the GCC box-like P box and the GCC box (Shoji et al. 2013, **Supplementary Table S7**). Accordingly, we used *in silico* analysis to identify P box and GCC box elements within the 1,500-bp 5'-flanking regions of *DWF5* and *GAME4*. Using a cutoff score of 7.0, two P boxes (named D1 and D2) in *DWF5* and one P box (named G1) encompassing a GCC box in *GAME4* were predicted, while no GCC box other than the one included in G1, was found. Both D1 and D2 were present within the short functional region (-285 to -1) of *DWF5*.

To clarify the role of the predicted elements in the *JRE4*-dependent reporter activation, nucleotides within the elements were substituted (**Fig. 6a**) and the resultant mutant reporters were subjected to transient transactivation assays (**Fig. 6b**). For *DWF5*, mutations in D1 abolished the *JRE4*-dependent activation of the reporter driven by the short region (-285 to -11). Mutations in D2, which resides in 5'-untranslated region rather than the promoter, did not have major influences on the induction, indicating the requirement of functional D1 element but not of D2. *GAME4* promoter activation did not change much

with mutations only in G1, suggesting the presence of additional elements indispensable for the promoter induction. Based on such assumption, we lowered the cutoff value in the analysis, and found the G2 element (-1111 to -1102) with score of 6.1 as a predicted P box (**Fig. 6a**). Mutations in G2 alone did not change activation, similar to those in G1 (**Fig. 6b**). However, when the *GAME4* promoter construct carried mutations at both G1 and G2, it was no longer activated by the *JRE4* effector, pointing the involvement of functionally redundant G1 and G2 in the *GAME4* activation.

To validate *in vitro* binding of the elements to JRE4 proteins, Electrophoretic Mobility Shift Assay (EMSA) was carried out with oligonucleotide probes based on sequences of the elements (**Supplementary Table S10**). When incubated with recombinant fusion proteins of truncated JRE4 (corresponding to 40 to 219 amino acids) tagged with N-terminal thioredoxin and other short tags, DNA-protein complexes were detected as intense shifted triplet bands for D2 and G1 probes (**Fig. 6c**). Similar patterns of shifted bands were observed for D1 and G2, albeit with lower intensity than those for the other two probes. Interestingly, the intensities of the shifted bands corresponded with the *in silico* prediction scores for the elements. The shifted bands were completely abolished when mutated probes (**Fig. 6a**) were used, confirming the specificity of binding of the wild-type probes.

**Putative JRE-binding elements found in proximal promoter regions of *JRE*-regulated**

**genes**

The JRE4-binding elements found in proximal promoter regions (**Fig. 6**), prompted us to examine whether genes with such JRE-binding elements in promoter regions were enriched among *JRE*-regulated genes. In addition to the P and GCC boxes targeted by clade 2-2b JRE4, a related CS1 box, recognized by clade 2-3 JREs (**Fig. 7a**), was included in the analysis. All of the examined boxes were represented as weighted matrices (**Supplementary Table S7**). We computationally searched for P, GCC, and CS1 boxes with a cut-off score of 7.0 in promoter regions (up to -800; counted from first ATG) of *JRE*-regulated genes (group R) (180 genes in **Supplementary Table S4**) and of *JRE*-regulated SGA biosynthesis genes, (group SR) (24 genes in **Fig. 3**), a subset of group R genes. The corresponding regions of all protein-coding genes annotated in a tomato reference genome (group W) (34,725 genes) were analyzed as controls. The genes with the JRE-binding elements in each group were counted. The values even for group W were slightly variable among examined regions, possibly reflecting biased GC-contents or other genomic features in promoter regions. We detected enrichment of genes with a P box in the -200 to -100 region for both R (2.1-fold) and SR groups (5.8-fold) and of genes with a CS1 box in the -300 to -1 region for group R (2.2- to 2.7-fold) and in the -300 to -200 region for group SR (5.7-fold).

To examine whether sequences related to P, GCC, and CS1 boxes could be retrieved in non-targeted analysis, the 5'-flanking sequences (-1500 to -1) of group R and SR genes

were subjected to MEME (Multiple Em for Motif Elicitation) analysis (Bailey et al. 2006), retrieving the sequences shared among the queries. Multiple sequences with similarity to the JRE-binding boxes were retrieved (**Supplementary Table S8**); match scores representing the similarities were calculated using position-specific probability matrices for P, GCC, and CS1 boxes based on sequences retrieved from the 5'-flanking regions (-300 to -1) of group R genes (**Supplementary Table S7**).

## *Discussion*

### Impacts of altered *JRE* function on SGA biosynthesis

Here, we used transgenic approaches, involving overexpression and dominant suppression, to elucidate the regulatory functions of tomato JRE transcription factors, which are closely related to alkaloid-regulating ORCA3 from *C. roseus* (van der Fits and Memelink 2001) and ERF189 from tobacco (Shoji et al. 2010). Based on microarray analyses, we identified a large number of *JRE*-regulated metabolic genes involved in SGA biosynthesis, including all clustered *GAME* genes except *GAME2*, constituting a core pathway downstream of cholesterol (Itkin et al. 2011, Itkin et al. 2013), genes for cholesterol biosynthesis, including *SSR2* (Sawai et al. 2014) and flux-controlling *HMGR* (Narita and Gruissem 1989), and others involved in the mevalonate pathway (**Fig. 2**). Our results demonstrate the existence of

*JRE*-mediated transcriptional regulation of the entire SGA pathway in tomato. This regulation of the upstream pathways, as far up as the isoprenoid-producing branch, may be required to meet the metabolic demands for downstream SGA production without disturbing homeostasis of other metabolites derived from the highly branched terpenoid pathways. The relatively small changes in the accumulation of the essential phytosterols (Boutté and Grebe 2009) campesterol and stigmasterol in the transgenic lines support this conclusion (**Fig. 4**). Although the overall pathway to SGA biosynthesis was generally coordinated, expression levels of genes involved in later steps, such as *GAME*s, changed much more in the transgenic lines than did the upstream genes (**Fig. 3**, **Fig. 4a**, **Supplementary Figure S4, Supplementary Table S2**, **Supplementary Table S3, Supplementary Table S5**). Such differential regulation between distinct parts of the pathway was corroborated with the changes in the levels of metabolites; changes in SGAs and upstream intermediates, cholesterol, cycloartenol, lanosterol, and squalene, showed opposite trends in both the overexpression and the suppression lines (**Fig. 5**). This difference in accumulation presumably reflects imbalances between the early and late parts of the pathway. To understand the metabolic changes of triterpenoids, α-amyrin, β-amyrin, and lupeol, which showed a trend opposite to that of cycloartenol and lanosterol (**Fig. 5**), it might be useful to examine the regulation of *oxidosqualene cyclase* genes, none of which were identified as the regulated genes in our microarray analysis. Of course, to better understand the metabolic impacts of

*JRE4* overexpression, we need to examine not only the expression of the metabolic genes at transcript level but also activities of the involved enzymes and metabolic flux reflecting them.

Our microarray-based approach to screening genes involved in a *JRE*-controlled regulon not only points to known structural genes (**Fig. 3**) but also helps mine novel metabolic and transport genes required for complex SGA-related metabolism. In this regard, it is intriguing that many uncharacterized genes annotated as encoding glucosyltransferases, cytochrome P450 enzymes, and peptide transporters were included in the list of *JRE*-regulated genes (**Supplementary Table S4**). Similar transgenic approaches combined with transcript profiling in other species producing SGAs are considered useful to elucidate the molecular bases of chemically diverse metabolites of this group (Friedman 2002, Friedman 2006, Iijima et al 2013). It should be noted that Cárdenas et al. (2016) recently reported that potato GAME9, an ortholog of tomato GAME9/JRE4, regulates the biosynthetic genes of the SGAs chaconine and solanine (Cárdenas et al. 2016). Our identification of a series of *JRE*-regulated metabolic genes in tomato provides new insights on cholesterol formation, which has been relatively unexplored in plants compared to other organisms (Sawai et al. 2013).

To understand this regulation in the context of a greater metabolic network, we will need to address the coordination of the *JRE*-mediated transcriptional regulation with other mechanisms operating at the transcriptional and post-transcriptional levels (Pollier et al. 2013,

Van Moerkercke et al. 2015, Mertens et al. 2015). As discussed below, it is still an open question whether all parts of the pathway are similarly subjected to the transcriptional regulation by *JRE*s. In addition to structural genes, molecular factors important for the pathway regulation could be included in the *JRE*-regulated genes. Notably, among the genes identified as regulated by *JRE*s (**Supplementary Table S**4) was a gene encoding a RING-finger E3 ubiquitin ligase, a homolog of MAKIBISH1 from *Medicago truncatula* that controls HMGR enzyme activity (Pollier et al. 2013). Studies of tomato *JRE*s and *GAME9* (Cárdenas 2016; this study), along with recent studies on a group of related bHLH transcription factors (Van Moerkercke et al. 2015, Mertens et al. 2015), open a new chapter in the study of the regulation of terpenoid pathways, which had been remained unexplored until recently.

**Transcriptional regulation of SGA biosynthesis genes**

JRE4 directly activates the transcription of *DWF5* and *GAME4* genes by recognizing the GCC-like elements in their promoter regions (**Fig. 6**). Two of the three functional elements found in *DWF5* and *GAME4* are present in similarly situated proximal regions (-248 to -219 relative to the ATG) (**Fig. 6a**). This finding is consistent with previous reports on ORCA3- and ERF189-recognizing elements present in similar regions of the targeted genes (van der Fits and Memelink 2000, Shoji et al. 2010, Shoji and Hashimoto 2011a) and also with the

computational predictions of the elements in the *JRE*-regulated genes (**Fig. 7**), suggesting a common mechanistic feature among transcription factors of this group. Our results for *GAME4*, which is present in a two-gene metabolic cluster (**Fig. 6**), point to a role for promoter-binding transcription factors in the regulation of such clusters, possibly in addition to their proposed regulation at the chromosomal level (Wegel et al. 2009).

It remains to be addressed whether all *JRE*-regulated SGA biosynthesis genes, including clustered *GAME*s other than *GAME4*, are regulated directly by *JRE*s in a similar manner as demonstrated for *DWF5* and *GAME4*. Considering the large number of regulated steps and the differential regulation we observed, we cannot exclude the possibility of the involvement of additional mechanisms, such as indirect regulation through other transcription factors or metabolite-mediated feedback regulation. As demonstrated for regulation of nicotine biosynthesis genes by ERF189 and the JAZ-interacting bHLH transcription factor MYC2 (Shoji and Hashimoto 2011b), it is also plausible that JREs regulate the downstream genes in cooperation with other transcription factors. In this regard, it is interesting that both MYC2 and GAME4/JRE4 were required for transactivation of promoters of SGA biosynthesis genes in tobacco cells (Cárdenas et al. 2016). Nevertheless, the significant enrichment among the *JRE*-regulated genes of those bearing a P or CS1 box in the proximal promoter (**Fig. 7**) and the complementary results of the MEME analysis (**Supplementary Table S8**) suggest that JRE4 and possibly other JREs, including clade 2-3 members that can

recognize the CS1 box, participate in the transcriptional regulation of many, but not necessarily all, of the genes by binding to the predicted elements. The frequent occurrence of the JRE-binding elements in the regulated genes supports the notion that genes acting downstream are recruited into regulons under the control of transcription factors through acquisition of functional *cis*-elements in the appropriate promoter regions (Shoji and Hashimoto 2011a, Moghe and Last 2015).

The results of our promoter-related analyses (**Fig. 6, Fig. 7**, **Supplementary Table S8**) point the possible importance of GCC-like P and CS1 boxes rather than the canonical GCC box for *JRE*-mediated regulation, although all JREs presumably have substantial *in vitro* binding abilities to GCC box (**Fig. 7a**, Shoji et al. 2013). As proposed for tobacco ERF189, which exclusively targets the P box (Shoji et al. 2013), such preference for the GCC-like box of JREs may allow the *JRE*-controlled regulon to be free from influence by the large number of GCC box-recognizing ERFs.

**Regulatory function of multiple *JRE* genes**

Gene clustering is common to *JRE*s (**Fig. 1a**) and related *ERF*s (Shoji et al. 2013); in tobacco, *ERF189* is clustered with related genes on a nicotine-controlling *NIC2* locus and the *NIC2*-locus cluster was found to be deleted in a low-nicotine mutant (Shoji et al. 2010), while *ORCA3* was found to reside on a same genomic contig with a similar gene in *C. roseus*

(Kellner et al. 2015). When overexpressed in a low-nicotine mutant, *ERF189* recovered nicotine accumulation to the wild-type levels, and thus *ERF189* has been considered to work most effectively as a regulator of nicotine biosynthesis among the clustered *ERF*s (Shoji et al. 2010). Similar to the *NIC2*-locus cluster in tobacco, the tomato *JRE* cluster includes members of different clades, namely clades 2-2b and 2-3 (**Fig. 1**). Dominant suppression of clade 2-2b *JRE3*, 2-2b *JRE4*, or 2-3 *JRE5* similarly repressed the expression of SGA biosynthesis genes (**Fig. 3, Supplementary Fig. S3**), suggesting overlapping functions of the three *JRE*s. Of course, the effects of ectopic expression of the dominant repressive forms of these proteins should be interpreted carefully. The involvement of clade 2-3 *JRE*s in SGA regulation is also supported by the frequent occurrences of CS1 boxes in promoters of the regulated genes. In addition to overexpression (**Fig. 3, Supplementary Fig. S4, Supplementary Table S2**) and promoter binding (**Fig. 6**) analyses as performed herein for *JRE4*, knock-out or knock-down experiments for individual members would be required to confirm the *in planta* contributions of each *JRE* to SGA regulation.

The gene expression patterns strongly support a role for *JRE4* in SGA regulation (**Fig. 2**). *JRE4* is expressed the most highly among *JRE*s at the transcript level and, as pointed in Itkin et al. (2013), its expression is clearly coordinated with SGA biosynthesis genes in various samples (**Fig. 2**). In fruits, progressive decreases of expression were evident for *JRE4* and *SMO1* and *GAME1* during the green fruit stages (**Fig. 2b**), indicating that SGA

formation mainly declines during the green stages rather than later color-changing stages (Iijima et al. 2009). In hairy roots, all *JRE*s were clearly induced by MeJA treatment, but their induction patterns were variable between the members (**Fig. 2c**). Again, the gradual induction of *JRE4* paralleled those of SGA biosynthesis genes during the 24-h duration of treatment. According to the co-expression analysis and other evidence, we can infer that one or few select members, such as tomato *JRE4*, tobacco *ERF189*, and possibly *C. roseus ORCA3*, play a predominant role in regulation of targeted metabolic pathways in each species. We need to further understand functional redundancy and divergence among the multiple *ERF* members to address why these *ERF* genes are maintained in a form of gene clusters during plant evolution.

**SGAs as defense chemicals in tomato**

Plants usually adapt particular classes of metabolites for chemical defense. A variety of compounds, including SGAs, methyl ketones, and sesquiterpenes, are considered to mediate the herbivore resistance in *Solanum* species (Antonious et al. 2014). SGAs are a group of bioactive compounds with abilities to bind to cholesterol, disrupt cellular membranes and inhibit cholinesterases (Friedman 2015). Based on their toxic and pharmacological properties, SGAs has been proposed to be involved in plant host resistance against a wide range of biotic agents, such as bacteria, fungi, virus, insects and animals (Friedman 2002,

Friedman 2006). A series of genes encoding biosynthetic enzymes and transcription factors involved in SGA biosynthesis were induced by MeJA treatment in tomato tissues (**Fig. 2c**, **Fig. 4a, Supplementary Fig. 1S, Supplementary Fig. 4S**). The JA-induced expression of the genes and involvement of tomato homologs of *ORCA3* and *ERF189* in their induction underline the committed roles of SGAs and JA signaling in induced chemical defense against herbivores in tomato, as in the case of nicotine in tobacco (Baldwin 1998, Shoji and Hashimoto 2013). Although induced significantly after elicitation, SGAs and nicotine are substantially produced even at basal levels and the amounts of SGA and nicotine accumulation in the tissues seem in a similar range (in orders of mg per g dry weight), indicating the similarities of these two alkaloid groups with analogous regulatory mechanisms. Drastic declines of expression of SGA biosynthetic and regulatory *JRE* genes during early fruit development in tomato (**Fig. 2c**) are an example of developmental regulation of defense chemical pathways, which may operate more generally, ensuring the removal of toxic substances from seed-bearing mature fruits to allow seed dispersal assisted by fruit-eating herbivores.

One of the main goals in tomato and potato breeding is the removal of toxic and anti-nutritional SGAs, which are not critically required for plant protection during normal cultivation and occasionally cause poisoning. The removal of SGAs becomes critical when considering the introduction of desirable genetic traits into cultivated species from wild

counterparts that usually produce SGAs at higher levels (Iijima et al. 2013). Our identification of the transcriptional regulators of SGA pathway provides a promising molecular tool applicable for the generation of the crops with low-SGA contents.

## *Materials and Methods*

### Plant growth, transformation and treatment

Sterilized seeds of tomato, *Solanum lycopersicum* cv. Micro-Tom, were germinated and grown to seedlings on half-strength Gamborg B5 medium solidified with 0.6% (w/v) agar and supplemented with 2% (w/v) sucrose. Two-week-old seedlings were transferred onto soil in pots and grown to maturity in the greenhouse.

The coding region of *JRE4* was cloned into the *Bam*HI and *Sac*I sites on pBI121 to generate a binary vector *p35S::JRE4* for overexpression. The *p35S::JRE4* vector was introduced into *Agrobacterium tumefaciens* strain GV2260 by electroporation. *Agrobacterium*-mediated transformation to generate transgenic tomato plants was done according to Sun et al. (2006). Shoots were selected on solidified Murashige and Skoog medium containing 100 mg liter$^{-1}$ kanamycin. Diploid individuals were screened in $T_0$ generation. Transgenic plants of the $T_3$ generation were analysed.

For gene expression analyses, leaves and roots from 4-week-old plantlets grown in greenhouse were submerged in B5 medium with 100 μM MeJA and incubated for 24 h in the

dark. Four individual 7-week-old plants were placed in air-tight plastic containers (ca. 81 liters in volume), with a cotton sheet soaked with 5 ml of 100 μM MeJA. The cotton sheet was replaced with a newly soaked one every day during the duration of treatment. Leaves detached from plants exposed to MeJA vapour for 4 d were used for metabolite analysis.

To generate the dominant-suppression vectors, coding sequences of *JRE3*, *JRE4*, and *JRE5* were amplified by PCR with primers including the restriction sites and a sequences for EAR motif (5'-CGGCCGCTTGATTTGGATCTTGAACTCAGACTTGGATTTGCTTA-3'; encoding LDLDLELRLGFA; Hiratsu et al., 2003) and inserted into the *Xba*I and *Sac*I sites of pBI121. To generate transgenic hairy roots, tomato hypocotyls from 7-day-old seedlings were infected with *Agrobacterium rhizogenes* strain ATCC15834 harboring a binary vector by briefly touching one end of hypocotyl segment (1.5 cm in length) to a bacterial colony and then standing the segments on the same agar medium with the contacted end up. Hairy roots emerging from infected sites were excised and subcultured twice every week on solidified B5 medium containing 300 mg liter$^{-1}$ cefotaxime for disinfection and 50 mg liter$^{-1}$ kanamycin for drug-resistance selection. The selected lines were maintained by subculturing every week in 125-ml glass flasks filled with 25 ml liquid B5 medium supplemented with 2% (w/v) sucrose with shaking at 100 rpm in the dark. MeJA was directly added to 4-day-old cultures to a final concentration of 100 μM.

**cDNA microarray analysis**

Total RNA was isolated from leaves treated with MeJA for 24 h and hairy roots treated with MeJA for 24 h using an RNeasy kit (Qiagen). RNA integrity was checked with an Agilent 2100 Bioanalyzer (Agilent). Total RNA (500 ng) was used to generate Cyanine 3-labelled cRNA probes using a Quick Amp Labeling Kit, One-Color (Agilent). A tomato custom oligoarray with 60-mer probes of more 40,000 sequences, designed using transcript sequences of the Tomato Gene Index Version 11 (LeGI v.11; http://www.danafarber.org/), was hybridized with the labelled samples and scanned, and data were captured and processed as described (Ruiu et al. 2015). Due to poor labelling, hybridization was cancelled for sample from *JRE4-EAR* line #2.

Probes with low signal intensity (averages for the two controls <0.2) and intensities variable between lines (differences between the two controls >2.5 folds) were excluded from the analysis. Values relative to the controls were obtained by pairwise comparisons and averaged for each construct; values were defined as $R_{ox}$, $R_{j3}$, $R_{j4}$, and $R_{j5}$ derived from data for *JRE4-OX*, *JRE3-EAR*, *JRE4-EAR*, and *JRE5-EAR* lines, respectively. For the overexpression experiment, probes with $R_{ox}>5$ are listed in **Supplementary Table S2**. For the suppression experiment, Q was defined as $Q^2=R_{j3}^2+R_{j4}^2+R_{j5}^2$ and probes with $Q<0.85$ are listed in **Supplementary Table S3**.

**qRT-PCR**

Total RNA was isolated from plant samples that had been ground in liquid nitrogen using RNeasy kit (Qiagen) and then converted to first-strand cDNA using ReverTra Ace qPCR RT Master Mix (Toyobo) with oligo(dT) primer. The cDNA templates were amplified using a LightCycler 96 (Roche) with SYBR Premix Ex Taq (Takara) according to Shoji et al. (2010). The primer sequences are given in **Supplementary Table S9**. *EF1α* (Solyc05g005060) was used as a reference gene. Each assay was repeated at least three times. Based on amplifications from equal molar quantities of cloned amplicons, amplifications from different primer pairs were normalized.

**Metabolite analysis**

For measurement of SGAs, freeze-dried samples (2 mg) were extracted with 250 μl (for hairy root samples) or 500 μl (for leaf samples) of 80% (v/v) methanol containing 2.5 μM lidocaine and 2.5 μM 10-camphour sulfonic acid using a mixer mill with zirconia beads for 7 min at 18Hz and 4°C. After centrifugation for 10 min at 12,000 *g*, the supernatant was filtered using an HLB μElution plate (Waters). The extracts (1 ul) were analyzed using LC-QTOF-MS (LC, Waters Acquity UPLC system; MS, Waters Xevo G2 Q-Tof). Positive ion mode was used and analytical conditions were as follows: LC column, Acquity bridged ethyl hybrid (BEH) C18 (1.7 μm, 2.1 mm × 100 mm, Waters); solvent system, solvent A

(water including 0.1% formic acid) and solvent B (acetonitrile including 0.1% formic acid); gradient program, 99.5%A/0.5%B at 0 min, 99.5%A/0.5%B at 0.1 min, 20%A/80%B at 10 min, 0.5%A/99.5%B at 10.1 min, 0.5%A/99.5%B at 12.0 min, 99.5%A/0.5%B at 12.1 min and 99.5%A/0.5%B at 15.0 min; flow rate, 0.3 ml/min at 0 min, 0.3 ml/min at 10 min, 0.4 ml/min at 10.1 min, 0.4 min/min at 14.4 min and 0.3 ml/min at 14.5 min; column temperature, 40 °C; MS detection: capillary voltage, +3.0 keV, cone voltage, 25.0 V, source temperature, 120 °C, desolvation temperature, 450 °C, cone gas flow, 50 l/h; desolvation gas flow, 800 l/h; collision energy, 6 V; mass range, *m/z* 50–1500; scan duration, 0.1 sec; inter-scan delay, 0.014 sec; data acquisition, centroid mode; Lockspray (Leucine enkephalin): scan duration, 1.0 sec; inter-scan delay, 0.1 sec. MS/MS data were acquired in ramp mode using the following analytical conditions: (1) MS: mass range, *m/z* 50–1500;scan duration, 0.1 sec; inter-scan delay, 0.014 sec; data acquisition, centroid mode; polarity, positive/negative; and (2) MS/MS: mass range, *m/z* 50–1500; scan duration, 0.02 sec; inter-scan delay, 0.014 sec; data acquisition, centroid mode; polarity, positive/negative collision energy, ramped from 10 to 50 V. In this mode, MS/MS spectra of the top 10 ions (> 1000 counts) in an MS scan were automatically obtained. If the ion intensity was less than 1000, MS/MS data acquisition was not performed and moved to of next top 10 ions. Chemical assignment of SGAs was performed using the MS/MS spectra reported in Itkin et al. (2011). All SGA levels were calculated based on a calibration curve of α-tomatine (Tokyo Chemical Industry Co., Ltd., Tokyo), assuming the

same molar responses of SGAs.

For measurement of triterpenes, the extraction of plant tissues with added standards ([25,26,26,26,27,27,27-$^{2}H_7$]cholesterol (98% D, Cambridge Isotope Laboratories, Inc., Andover, MA, USA) or synthesized [3,28,28,28-$^{2}H_4$] β-amyrin, [28,28,28-$^{2}H_3$] α-amyrin, and 28,28,28-$^{2}H_3$] lupeol (Ohyama et al. 2007)) was carried out using the method previously described (Tsukagoshi et al, 2016). Quantification of triterpenes except for lanosterol and squalene using GC-MS analysis was performed as described previously (for sterols; Choi et al, 2014, for triterpenols; Ohyama et al. 2007). Lanosterol amounts were calculated using the peak area ratio of fragment ion (*m/z*: 393) of trimethylsilylated lanosterol and that (*m/z*: 336) of the standard (TMS derivative of the labeled cholesterol). Quantification of squalene was performed using the standard calibration curve with coefficients of determination, $r^2 > 0.9996$. The curves were constructed using the peak area value of TIC (total ion chromatogram).

**Transactivation assay**

The 5'-flanking regions of *DWF5* and *GAME5* were amplified by PCR from tomato genomic DNA with primers attached with the restriction sites and cloned into the *Hin*dIII and *Bam*HI sites on pBI121 to generate the *GUS* reporter constructs. For mutant reporter constructs, before cloning the fragments into pBI121, PCR-based mutagenesis (Hemsley et al. 1989) was used to substitute the nucleotides in the cloned promoter sequences; nucleotide substitutions

introduced are shown in **Fig. 6a**. *pGBW17* was used as the empty-vector control for the effector plasmids. The binary vectors, *p19s* for P19 silencing suppressor (Voinnet et al. 2003) and *p35S-GFP* for *GFP* reference gene, were used.

Transient gene expression was performed in tomato fruits according to an agroinjection protocol (Orzaez et al. 2006). Briefly, *Agrobacteriun tumefaciens* strain EHA105 with a binary vector was grown overnight in YEB medium supplemented with 20 μM acetosyringone and appropriate antibiotics and recovered by centrifugation at 4,000 *g* for 20 min. The cells were re-suspended in infiltration buffer (10 mM MES, 10 mM $MgCl_2$, 200 μM acetosyringone, pH 5.7) by adjusting optical density at 600 nm to 0.25, and then incubated for at least 2 h at room temperature in the dark. The bacterial suspensions for reporter and effector vectors plus those for *p19s* and *p35S-GFP* vectors were combined, and the resultant solution (200 to 300 μl per fruit) was injected into mature green fruits (1 to 1.5 cm in size) using a 1-ml plastic syringe attached to a 27-gauge needle. Gene expression was analyzed by qRT-PCR using fruits harvested 3 d after the injection.

**EMSA**

Bacterial expression and purification of recombinant fusion proteins of JRE4, called Sl1g90340 in Shoji et al. (2013), were done as described (Shoji et al. 2013). In the pET32b-based expression vector, a portion of *JRE4* (corresponding to 40-219 amino acid

residues) was placed downstream of a sequence for N-terminal tags, a thioredoxin, an S-tag, and a His-tag (Shoji et al. 2013). Proteins comprising only with the tag portion from empty pET32b were purified and used as the controls.

Sequences of sense and antisense oligonucleotides used are given in **Supplementary Table S10**. Probe preparation, DNA-protein-binding assays, gel separation, and detection of the reaction products were carried out as described (Shoji et al. 2010).

**Computational analysis**

We used Regulatory Sequence Analysis Tools (RSAT; Turatsinze et al. 2008, http://rsat.ulb.ac.be/rsat/) to search for putative JRE binding elements in the query genomic sequences by weight matrix scoring. Weight matrices for the P, GCC, and CS1 boxes (Shoji et al. 2013) are given in **Supplementary Table S7**. The default setting were used for all parameters. Elements with scores higher than 7.0 were retained for analysis, along with element G2, which had a score of 6.1 in *GAME4*. Genes with putative JRE-binding elements in the examined regions were counted. Significant differences of the values compared to those of group W including all tomato protein coding genes was determined by one-sided Fisher's exact test ($\alpha$=0.05) using the fisher test function of R (V. 3.2.2).

Based on sequences predicted to be the JRE-binding elements by RSAT in the regions (-300 to -1) of group R genes, position-specific probability matrices for P, GCC, and

CS1 boxes (**Supplementary Table S7**) were generated by MEME software (v. 4. 10. 2., Bailey et al. 2006) with option settings; '2' for '-nmotif', '10' for '-minw' and applying '-revcomp'. To retrieve the sequences commonly found in the queries, MEME was used with option settings; '10' for '-nmotif', '7' for '-minw' and applying '-revcomp'. Match scores representing the similarities between a pair of the retrieved sequence and the JRE-binding box (P, GCC, or CS1) were calculated using position-specific probability matrices for the pairs. When a pair of sequences with lengths of $L_1$ and $L_2$ were aligned with the overlapping length of $L_3$, the alignment length Le was defined as $Le=L_1+L_2-L_3$. Differences between 1 and normalized vector distances were summed for overlapping positions and divided by Le to give scores for the alignments. The alignment scores were calculated for all possible alignments with no gap in both orientations for a sequence pair, and the highest alignment score was adapted as match score for the pair.

## Supplementary data

**Figure S1** Transgenic *JRE4-OX* tomato plants.

**Figure S2** Expression levels of *JRE* genes in transgenic *JRE-EAR* hairy root lines.

**Figure S3** Venn diagram showing the numbers of probes down-regulated (Rj3<0.4 for *JRE3-EAR*, Rj4<0.4 for *JRE4-EAR*, Rj5<0.4 for *JRE5-EAR*) by each *JRE-EAR*.

**Figure S4** Gene expression in roots of transgenic *JRE4-OX* tomato plants.

**Figure S5** Schematic diagram of SGAs in their biosynthetic pathway.

**Table S1** Transcript levels of *JRE* genes and SGA biosynthesis genes in tomato tissues.

**Table S2** Probes up-regulated in *JRE4-OX* lines.

**Table S3** Probes down-regulated in *JRE-EAR* lines.

**Table S4** *JRE*-regulated genes.

**Table S5** Signal intensities of probes corresponding to *JRE*-regulated SGA biosynthesis genes

**Table S6** SGA levels in transgenic tomato *JRE4-OX* plant and *JRE4-EAR* hairy root lines.

**Table S7** Matrices for P box, GCC box, and CS1 box.

**Table S8** Top 10 sequences retrieved by MEME analysis.

**Table S9** Oligonucleotide primers used for qRT-PCR analysis.

**Table S10** Sense and anti-sense oligonucleotides for probes used in EMSA

***Funding***

This work was supported by a Grant-in-Aid for Scientific Research (C) [grant number 26440144] from the Japan Society for the Promotion of Science to T.S. and Cooperative Research Grant of the Plant Transgenic Design Initiative, Gene Research Center, University of Tsukuba.

***Disclosures***

The authors have no conflicts of interest to declare.

***Acknowledgements***

We thank Drs. Tsuyoshi Nakagawa and Yoshinori Yagi for providing *pGBW17* and *p35S-GFP*, respectively. This work was supported in part by the RIKEN Plant Transformation Network and the Japan Advanced Plant Science Network.



***References***

Antonious, G.F., Kamminga, K., Snyder, J.C. (2014) Wild tomato leaf extracts for spider mite and cowpea aphid control. *J. Environ. Sci. Health B.* 49: 527-531.

Bailey, T.L., Williams, N., Misleh, C. and Li, W.W. (2006) MEME: discovering and analyzing DNA and protein sequence motifs. *Nucleic Acids Res.* 34: W369-373.

Baldwin, I.T. (1998) Jasmonate-induced responses are costly but benefit plants under attack in native populations. *Proc. Natl. Acad. Sci.* 95: 8113-8118.

Bednarek, P. and Osbourn, A. (2009) Plant-microbe interactions: chemical diversity in plant

defense. *Science* 324: 746-748.

Betz, J.M. (1999) Plant toxins. *J. AOAC Int.* 82: 781-784.

Boutté, Y. and Grebe, M. (2009) Cellular processes replying on sterol function in plants. *Curr. Opin. Plant Biol.* 12: 705-713.

Boycheva, S., Daviet, L., Wolfender, J.L. and Fitzpatrick, T.B. (2014) The rise of operon-like gene clusters in plants. *Trends in Plant Sci.* 19: 447-459.

Cárdenas, P.D., Sonawane, P.D., Pollier, J., Bossche, R.V., Dewangan, V., Weithorn, E. et al. (2016) GAME9 regulates the biosynthesis of steroidal alkaloids and upstream isoprenoids in the plant mevalonate pathway. *Nat. Comm.* 7:10654.

Choi H, Ohyama K, Kim YY, Jin JY, Lee SB, Yamaoka Y. et al. (2014) The role of Arabidopsis ABCG9 and ABCG31 ATP binding cassette transporters in pollen fitness and the deposition of steryl glycosides on the pollen coat. *Plant Cell* 26:310-24.

Crooks, G.E., Hon, G., Chandonia, J.M. and Brenner, S.E. (2004) WebLogo: a sequence logo

generator. *Genome Res.* 14: 1188-1190.

De Geyter, N., Gholami, A., Goormachtig, S. and Goossens, A. (2012) Transcriptional machineries in jasmonate-elicited plant secondary metabolism. *Trends Plant Sci.* 17: 349-359.

Friedman, M. (2002) Tomato glycoalkaloids: role in the plant and in the diet. *J. Agric. Food Chem.* 50: 5751-5780.

Friedman, M. (2006) Potato glycoalkaloids and metabolites: roles in the plant and in the diet. *J. Agric. Food Chem.* 54: 8655-8681.

Friedman, M. (2015) Chemistry and anticarcinogenic mechanisms of glycoalkaloids produced by eggplants, potatoes, and tomatoes. *J. Agric. Food Chem.* 63: 3323-3337.

Hemsley, A., Amheim, N., Toney, M.D., Cortpassi, G. and Galas, D.J. (1989) A simple method for site-directed mutagenesis using the polymerase chain reaction. *Nucleic Acids Res.* 17: 6547-6551.

Hiratsu, K., Mitsuda, N., Matsui, K. and Ohme-Takagi, M. (2003) Dominant repression of

target genes by chimeric repressors that include the EAR motif, a repression domain, in Arabidopsis. *Plant J.* 34: 733-739.

Iijima, Y., Fujiwara, Y., Tokita, T., Ikeda, T., Nohara, T., Aoki, K. et al. (2009) Involvement of ethylene in the accumulation of esculeoside A during fruit ripening of tomato (*Solanum lycopersicum*). *J. Agric. Food Chem.* 57: 3247-3252.

Iijima, Y., Watanabe, B., Sasaki, R., Takenaka, M., Ono, H., Sakurai, N. et al. (2013) Steroidal glycoalkaloid profiling and structures of glycoalkaloids in wild tomato fruit. *Phytochemistry* 95: 145-157.

Itkin, M., Heinig, U., Tzfadia, O., Bhide, A.J., Shinde, B., Cardenas, P. et al. (2013) Biosynthesis of antinutritional alkaloids in Solanaceous crops is mediated by clustered genes. *Science* 341: 175-179.

Itkin, M., Rogachev, I., Alkan, N., Rosenberg, T., Malitsky, S., Masini, L. et al. (2011) GLYCOALKALOID METABOLISM1 is required for steroidal alkaloid glycosylation and prevention of phytotoxicity in tomato. *Plant Cell* 23: 4507-4525.

Kazan, K. and Manners, J.M. (2013) MYC2: The master in action. *Mol. Plant* 6: 686-703.

Kellner, F., Kim, J., Clavijo, B.J., Hamilton, J.P., Childs, K.L., Vaillancourt, B. et al. (2015) Genome-guided investigation of plant natural product biosynthesis. Plant J. 82: 680-692.

Mertens, J., Pollier, J., Vanden Bossche, R., Lopez-Vidriero, I., Franco-Zorrilla, J.M. and Goossens, A. (2016) The bHLH transcription factors TSAR1 and TSAR2 regulate triterpene saponin biosynthesis in *Medicago truncatula*. *Plant Physiol.* 170: 194-210.

Moehs, C.P., Allen, P.V., Friedman, M. and Belknap, W.R. (1997) Cloning and expression of solanidine UDP-glucose glucosyltransferase from potato. *Plant J.* 11: 227-236.

Moghe, G.D. and Last, R.L. (2015) Something old, something new: conserved enzymes and the evolution of novelty in plant specialized metabolism. *Plant Physiol.* 169: 1512-1523.

Nakano, T., Suzuki, K., Fujimura, T. and Shinshi, H. (2006) Genome-wide analysis of the ERF gene family in Arabidopsis and rice. *Plant Physiol.* 140: 411-432.

Narita, J.O. and Gruissem, W. (1989) Tomato hydroxymethylglutaryl-CoA reduxtase is

required early in fruit development but not during ripening. *Plant Cell* 1: 181-190.

Ohyama K, Suzuki M, Masuda K, Yoshida S, and Muranaka T (2007) Chemical phenotypes of the *hmg1* and *hmg2* mutants of *Arabidopsis* demonstrate the in-planta role of HMG-CoA reductase in triterpene biosynthesis. *Chem. Pharm. Bull.* 55:1518-1521.

Orzaez, D., Mirabel, S., Wieland, W.H. and Granell, A. (2006) Agroinjection of tomato fruits. A tool for rapid functional analysis of transgenes directly in friut. *Plant Physiol.* 140: 3-11.

Pollier, J., Moses, T., González-Guzmán, M., De Geyter, N., Lippens, S., Vanden Bossche, R. et al. (2013) The protein quality control system manage plant defence compound synthesis. *Nature* 504: 148-152.

Ruiu, F., Picarella, M.E., Imanishi, S. and Mazzucato, A. (2015) A transcriptomic approach to identity regulatory genes involved in fruit set of wild-type and perthenocarpic tomato genotypes. *Plant Mol. Biol.* 89: 263-278.

Sawai, S, Ohyama, K., Yasumoto, S., Seki, H., Sakuma, T., Yamamoto, T. et al. (2014) Sterol side chain reductase 2 is a key enzyme in the biosynthesis of cholesterol, the common

precursor for toxic steroidal glycoalkaloids in potato. *Plant Cell* 26: 3763-3774.

Shoji, T. and Hashimoto, T. (2011a) Recruitment of a duplicated primary metabolism gene into the nicotine biosynthesis regulon in tobacco. *Plant J.* 67: 949-959.

Shoji, T. and Hashimoto, T. (2011b) Tobacco MYC2 regulates jasmonate-inducible nicotine biosynthesis genes directly and by way of the NIC2-locus ERF genes. *Plant Cell Physiology* 52: 1117-1130.

Shoji, T. and Hashimoto, T. (2013) Smoking out the masters: transcriptional regulators for nicotine biosynthesis in tobacco. *Plant Biotechnol.* 30: 217-224.

Shoji, T., Inai, K., Yazaki, Y., Sato, Y., Takase, H., Shitan, N. et al. (2009) Multidrug and toxic compound extrusion-type transporters implicated in vacuolar sequestration of nicotine in tobacco roots. *Plant Physiol.* 149; 708-718.

Shoji, T., Kajikawa, M. and Hashimoto, T. (2010) Clustered transcription factor genes regulate nicotine biosynthesis in tobacco. *Plant Cell* 22: 3390-3409.

Shoji, T., Mishima, M. and Hashimoto, T. (2013) Divergent DNA-binding specificities of a group of ETHYLENE RESPONSE FACTOR transcription factors involved in plant defense. *Plant Physiol.* 162: 977-990.

Sun, H.J., Uchii, S., Watanabe, S. and Ezura, H. (2006) A highly efficient transformation protocol for Micro-Tom, a model cultivar for tomato functional genomics. *Plant Cell Physiol.* 47: 426-431.

Tsukagoshi Y, Suzuki H, Seki H, Muranaka T, Ohyama K, and Fujimoto Y (2016) *Ajuga* $\Delta^{24}$-sterol reductase catalyzes the direct reductive conversion of 24-methylenecholesterol to campesterol. *J. Biol. Chem. in press*.

Tamura, K., Stecher, G., Peterson, D., Fillpski, A. and Kumar, S. (2013) MEGA6: molecular evolutionary genetic analysis version 6.0. *Mol. Biol. Evol.* 30: 2725-2729.

Thompson, J.D., Higgins, D.G. and Gibson, T.J. (1994) CLUSTAL W: improving the sensitivity of progressive multiple sequence alignment through sequence weighting, position-specific gap penalties and weight matrix choice. *Nucleic. Acid Res.* 22: 4673-4680.

Turatsinze, J.V., Thomas-Collier, M., Defrance, M. and van Helden, J. (2008) Using RSAT to scan genome sequences for transcription factor binding sites and *cis*-regulatory modules. *Nat. Proto.* 3: 1578-1588.

Van der Fits, L. and Memelink, J. (2000) ORCA3, a jasmonate-responsive transcriptional regulator of plant primary and secondary metabolism. *Science* 289: 295-297.

Van Moerkercke, A., Steensma, P., Schweizer, F., Pollier, J., Gariboldi, I., Payne, R. et al. (2015) The bHLH transcription factor BIS1 controls the iridoid branch of the monoterpenoid indole alkaloid pathway in *Catharanthus roseus*. *Proc. Natl. Acad. Sci. USA* 112: 8130-8135.

Voinnet, O., Rivas, S., Mestre, P. and Baulcombe, D. (2003) An enhanced transient expression system in plants based on suppression of gene silencing by the p19 protein of tomato bushy stunt virus. *Plant J.* 33: 949-956.

Wasternack, C. and Hause, B. (2013) Jasmonates: biosynthesis, perception, signal transdaction and action in plant stress response, growth and development. An update to the 2007 review in Annals of Botany. *Ann. Bot.* 111: 1021-1058.

Wegel, E., Koumproglou, R., Shaw, P. and Osbourn, A. (2009) Cell type-specific chromatin decondensation of a metabolic gene cluster in oats. *Plant Cell* 21: 3926-3936.

Yukimune, Y., Tabata, H., higashi, Y. and Hara, Y. (1996) Methyl jasmonate-induced overproduction of paclitaxel and baccatin III in Taxus cell suspension cultures. *Nat. Biotechnol.* 14: 1129-1132.

Zhang, H., Hedhili, S., Montiel, G., Zhang, Y., Chatel, G., Pré, M. et al. (2011) The basic helix-loop-helix transcription factor CrMYC2 controls the jasmonate-responsive expression of the *ORCA* genes that regulate alkaloid biosynthesis in *Catharanthus roseus*. *Plant J.* 67: 61-71.

***Legends to figures***

**Figure 1** Tomato *JRE* genes

(a) Schematic presentation of the cluster of five *JRE* genes on chromosome I and *JRE6* on chromosome V. *JRE* and other genes are represented as black and gray boxes, respectively. Strands on which each gene resides are indicated with arrowheads. (b) Phylogenetic tree of tomato JREs and related ERF proteins from Arabidopsis, *Catharanthus roseus*, and tobacco. Two clade 1 ERF proteins of group IXa, At ERF1 and At ERF2, were included as an outgroup.

Amino acid sequences of the DNA-binding domain were aligned using ClustalW (Thompson et al. 1994). An unrooted phylogenetic tree was constructed using the neighbor-joining algorithm with MEGA6 (Tamura et al. 2013). Bootstrap values are indicated at branch nodes, and the scale bar indicates the number of amino acid substitution per site. Species names are denoted with prefixes. At, Arabidopsis; Cr, *C. roseus*; Nt, tobacco; Sl, tomato.

**Figure 2** Expression patterns of *JRE* genes in tomato.

Tomato flower, leaf, stem, and root (a) and fruits of different ripening stages (b) were examined. Wild-type tomato hairy roots were treated by 100 μM MeJA for 0. 0.5, 1. 4, and 24h (c). Transcript levels were analyzed by qRT-PCR. Heat maps were drawn using average values (**Supplementary Table S1**) of three biological replicates. For *JRE*s, values are calculated relative to those of *EF1a*, and are shown relative to the value (set to 100, marked with asterisk) of *JRE4* in hairy roots treated by MeJA for 24 h. For *HMGR1*, *SMO1*, and *GAME1*, levels are shown relative to those in leaf, in fruit at stages with highest expression for each, or in hairy roots at 0 h.

**Figure 3** *JRE*-regulated SGA biosynthesis genes identified by cDNA microarray analysis.

Probes corresponding to SGA biosynthesis genes up-regulated by *JRE4* overexpression or down-regulated by dominant suppression of *JRE*s are shown. Signal intensities relative to

those of one of the controls (WT1 or VC1) are represented as heat maps (values available in **Supplementary Table S5**). Probes with $R_{ox}$>5 and Q<0.85 are marked with red and blue asterisks, respectively. Schematic view of SGA biosynthesis pathway is on the left. ACAA, acetyl-CoA *C*-acetyltransferase; HMGS, hydroxymethylglutaryl-CoA synthase; HMGR, 3-hydroxy-3-methylglutaryl CoA reductase: IDI, isopentenyl-diphosphate Δ-isomerase; SQO, squalene monooxygenase; SSR2, sterol side chain reductase 2; O14DM, obtsuifoliol 14α-demethylase; D14SR, Δ14-sterol reductase; SCDH, sterol-4α-carboxylate 3-dehydrogenase; HYD1, 3β-hydroxysteroid-Δ8Δ7-isomerase; SMO2, sterol 4α-methyl oxidase 2; DWF7, sterol C-5 desaturase; DWF5, sterol reductase; GAME, glycoalkaloid metabolism; IPP, isopentenyl pyrophosphate; DMPP, dimethylallyl pyrophosphate.

**Figure 4** Expression levels of SGA biosynthesis genes in transgenic tomato *JRE4-OX* plant and *JRE4-EAR* hairy root lines.

Transcript levels were analyzed by qRT-PCR. The error bars indicate the SD for three biological replicates. Levels are shown relative to the controls. See legend of **Fig. 3** for abbreviations of gene names. (a) Levels in leaves from *JRE4-OX* plant lines treated with MeJA for 24 h. (b) Levels in hairy roots of *JRE4-EAR* (line #1) treated with MeJA for 24 h.

**Figure 5** Metabolite levels in transgenic tomato *JRE4-OX* plant and *JRE4-EAR* hairy root

lines.

Metabolite levels were analyzed by LC-QTOF-MS for α-tomatine and by GC-MS for others. The error bars represent SD from four (for a) or five (for b) biological replicates. Levels of other SGAs are available in **Supplementary Table S6**. (a) Levels in leaves from *JRE4-OX* plants (line OX1) exposed to MeJA vapor for 4 d. (b) Levels in hairy roots of *JRE4-EAR* (line #1) treated with MeJA for 4 d. (c) Metabolites are schematically indicated in SGA biosynthesis pathway.

**Figure 6** *JRE4*-mediated activation of *DWF5* and *GAME4* is dependent on JRE-binding elements found in the promoter regions.

(a) Schematic representation of 5'-flanking regions of *DWF5* and *GAME4*. The positions of JRE-binding elements (arrowheads) and transcriptional start sites (arrows with vertical lines) are shown. On the right, nucleotide sequences of the elements are shown, while only the substituted nucleotides are indicated in mutated versions. (b) Transient transactivation assays in tomato fruits. *GUS* reporter gene fused with 5'-flanking regions of *DWF5* (-1,500 to -1 or -285 to -1; counted from the first ATG) and *GAME4* (-1,500 to -1) or their mutated versions, were delivered into tomato fruits by agroinjection with *JRE4* effector plasmid or empty vector (EV) and *GFP* reference plasmid. Expression levels of *GUS* reporter gene were normalized to those of the *GFP* reference gene, and are shown as relative values against

the values of each wild-type reporter with EV. The bars indicate SD from four independent experiments. Significant differences between EV and *JRE4* effector for each reporter were determined by Student's *t*-test: **P*<0.05; ***P*<0.01. (c) EMSA assay showing *in vitro* binding of recombinant JRE4 to the predicted elements. Probes were incubated with proteins from empty vector control or recombinant JRE4. Probe sequences are available in **Supplementary Table S10**.

**Figure 7** Computational prediction of putative JRE-binding elements in promoter regions of genes regulated by *JRE*s.

(a) Presumed binding elements of JREs. DNA-binding specificities of JRE4 and related ERFs from other species had been studied （Shoji et al. 2013）; the binding of JRE4 to P and GCC boxes was experimentally validated, while those for other JREs are presumed based on the results of clade 2-2b JRE4 for JRE3 and those of clade 2-3 ORCA3 from *C. roseus* for the remaining four JREs. Sequence logos representing P , CS1 , and GCC boxes were generated by WebLogo (Crooks et al. 2004) based on position-specific probability matrices (**Supplementary Table S7**), which were determined using the sequences predicted in the 5'-flanking regions (-300 to -1) of group R genes. (b) Genes predicted with JRE-binding elements (scores > 7.0) for indicated region in group W (black), R (blue) and SR (red). The genes of group R (180 *JRE*-regulated genes) and of group SR (*JRE*-regulated 24 SGA

biosynthesis genes) are given in **Supplementary Table S4** and **Fig. 3**, respectively. Significant differences of values (shown in %) from those for group W (all 34,725 protein-coding genes in tomato genome) were determined by one-sided Fisher's exact test; **P*<0.05, ***P*<0.01.

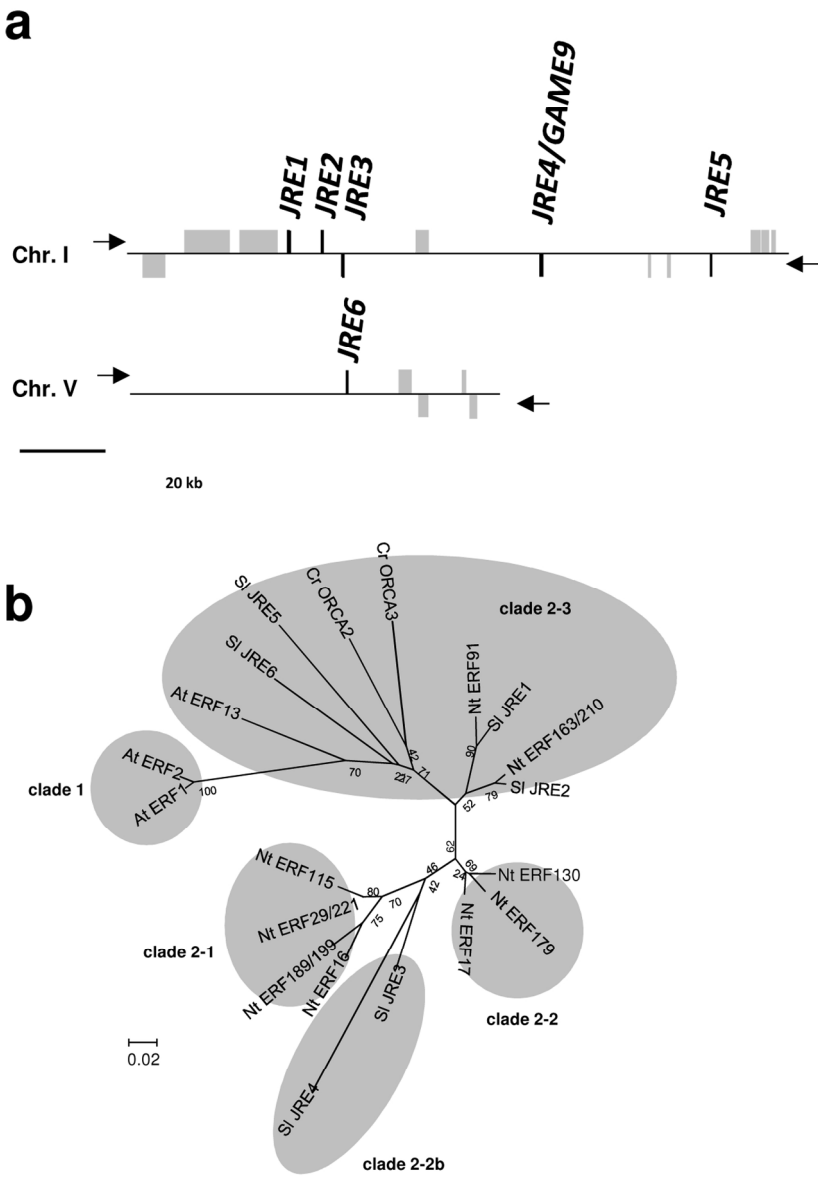


Figure 1 Tomato JRE genes

(a) Schematic presentation of the cluster of five JRE genes on chromosome I and JRE6 on chromosome V. JRE and other genes are represented as black and gray boxes, respectively. Strands on which each gene resides are indicated with arrowheads. (b) Phylogenetic tree of tomato JREs and related ERF proteins from Arabidopsis, Catharanthus roseus, and tobacco. Two clade 1 ERF proteins of group IXa, At ERF1 and At ERF2, were included as an outgroup. Amino acid sequences of the DNA-binding domain were aligned using ClustalW (Thompson et al. 1994). An unrooted phylogenetic tree was constructed using the neighbor-joining algorithm with MEGA6 (Tamura et al. 2013). Bootstrap values are indicated at branch nodes, and the scale bar indicates the number of amino acid substitution per site. Species names are denoted with prefixes. At, Arabidopsis; Cr, C. roseus; Nt, tobacco; Sl, tomato.

174x252mm (300 x 300 DPI)

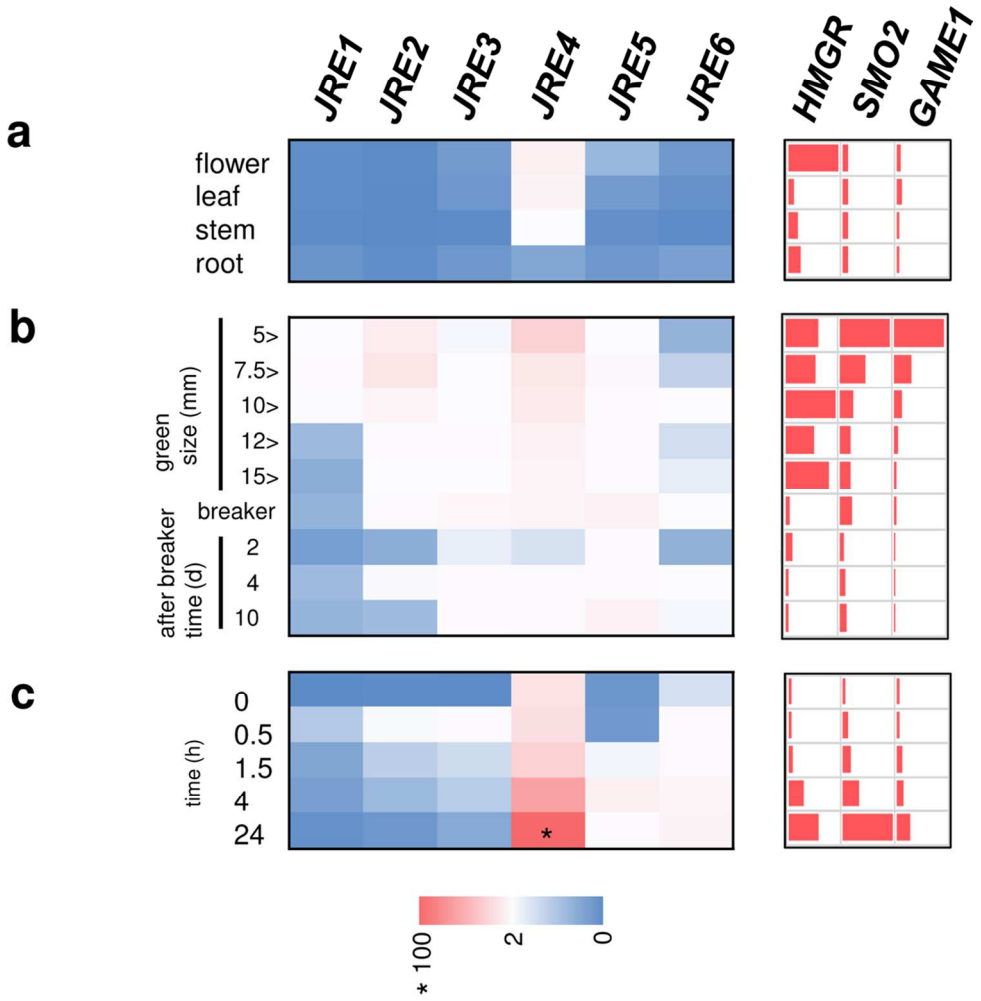


Figure 2 Expression patterns of JRE genes in tomato.
Tomato flower, leaf, stem, and root (a) and fruits of different ripening stages (b) were examined. Wild-type tomato hairy roots were treated by 100 μM MeJA for 0. 0.5, 1. 4, and 24h (c). Transcript levels were analyzed by qRT-PCR. Heat maps were drawn using average values (Supplementary Table S1) of three biological replicates. For JREs, values are calculated relative to those of EF1a, and are shown relative to the value (set to 100, marked with asterisk) of JRE4 in hairy roots treated by MeJA for 24 h. For HMGR1, SMO1, and GAME1, levels are shown relative to those in leaf, in fruit at stages with highest expression for each, or in hairy roots at 0 h.

119x122mm (300 x 300 DPI)

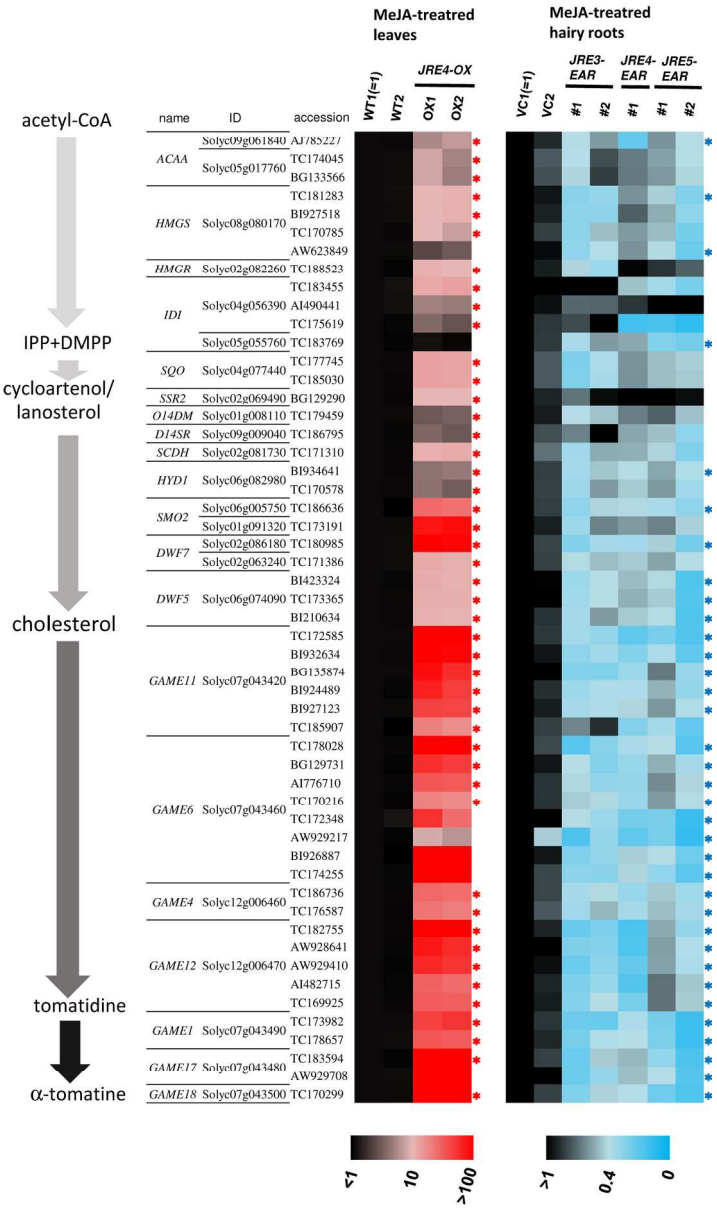


Figure 3 JRE-regulated SGA biosynthesis genes identified by cDNA microarray analysis. Probes corresponding to SGA biosynthesis genes up-regulated by JRE4 overexpression or down-regulated by dominant suppression of JREs are shown. Signal intensities relative to those of one of the controls (WT1 or VC1) are represented as heat maps (values available in Supplementary Table S5). Probes with Rox>5 and Q<0.85 are marked with red and blue asterisks, respectively. Schematic view of SGA biosynthesis pathway is on the left. ACAA, acetyl-CoA C-acetyltransferase; HMGS, hydroxymethylglutaryl-CoA synthase; HMGR, 3-hydroxy-3-methylglutaryl CoA reductase: IDI, isopentenyl-diphosphate Δ-isomerase; SQO, squalene monooxygenase; SSR2, sterol side chain reductase 2; O14DM, obtsuifoliol 14α-demethylase; D14SR, Δ14-sterol reductase; SCDH, sterol-4α-carboxylate 3-dehydrogenase; HYD1, 3β-hydroxysteroid-Δ8Δ7-isomerase; SMO2, sterol 4α-methyl oxidase 2; DWF7, sterol C-5 desaturase; DWF5, sterol reductase; GAME, glycoalkaloid metabolism; IPP, isopentenyl pyrophosphate; DMPP, dimethylallyl pyrophosphate.

209x345mm (300 x 300 DPI)

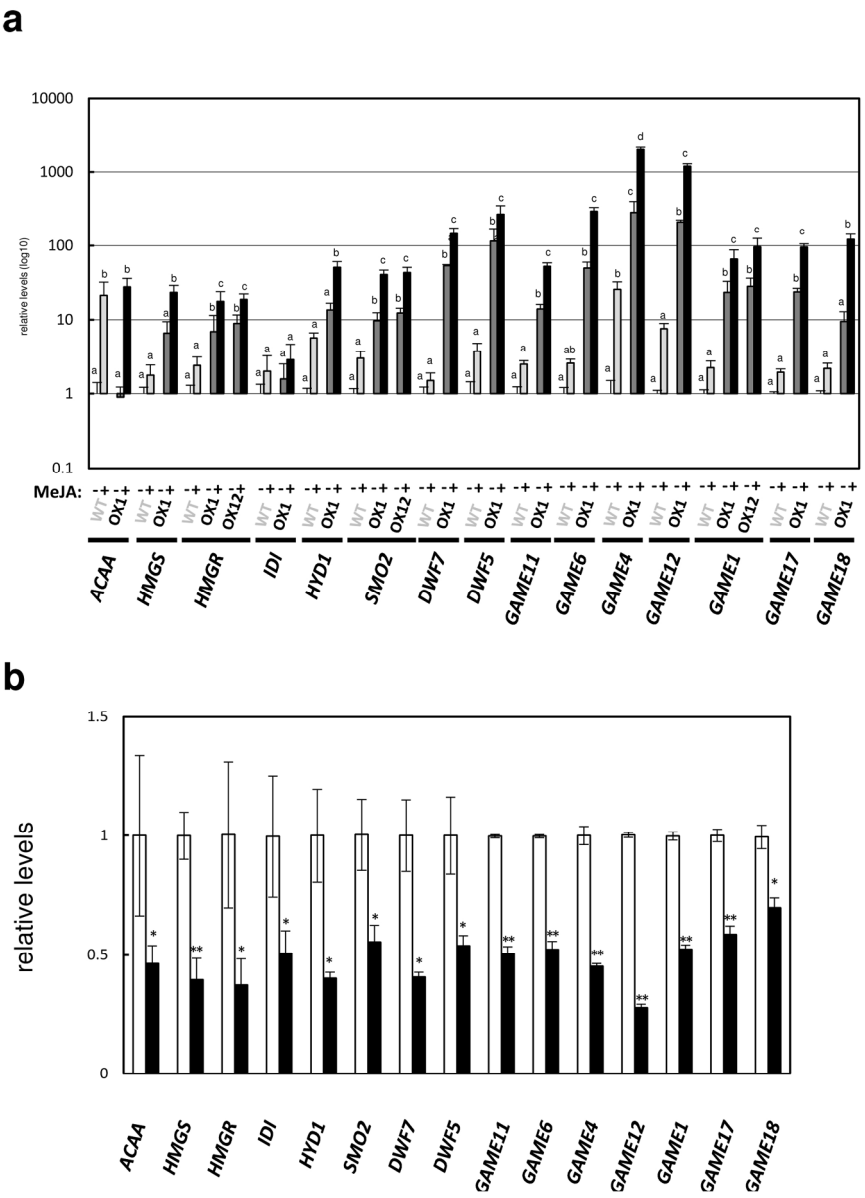


Figure 4 Expression levels of SGA biosynthesis genes in transgenic tomato JRE4-OX plant and JRE4-EAR hairy root lines.

Transcript levels were analyzed by qRT-PCR. The error bars indicate the SD for three biological replicates. Levels are shown relative to the controls. See legend of Fig. 3 for abbreviations of gene names. (a) Levels in leaves from JRE4-OX plant lines treated with MeJA for 24 h. (b) Levels in hairy roots of JRE4-EAR (line #1) treated with MeJA for 24 h.

209x283mm (300 x 300 DPI)

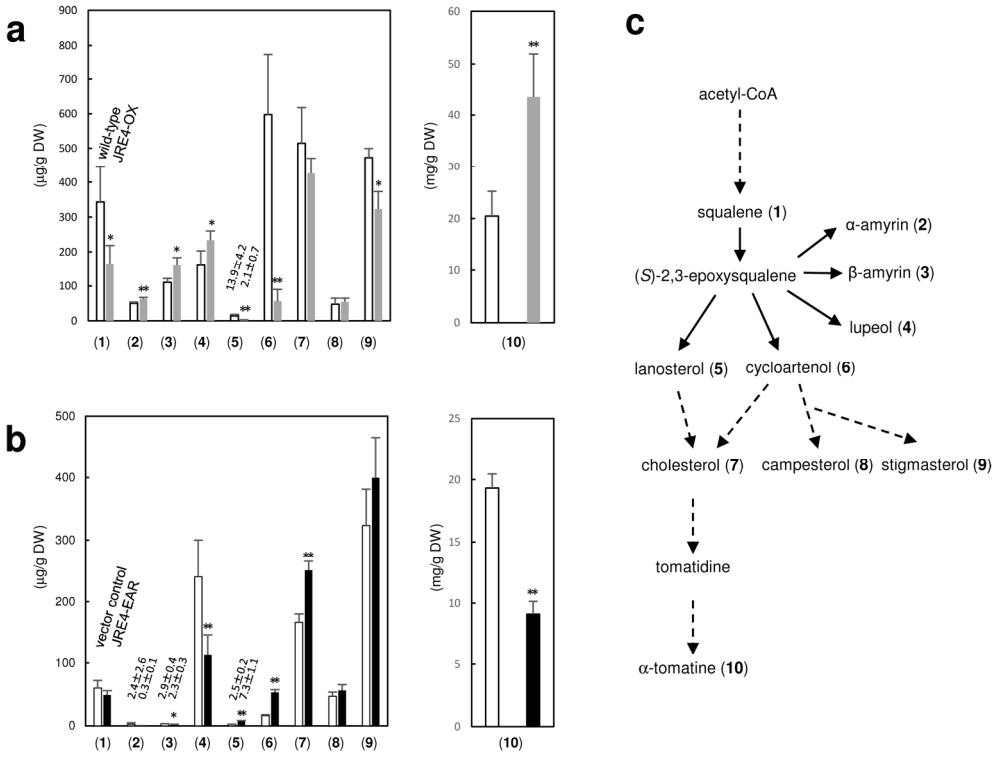


Figure 5 Metabolite levels in transgenic tomato JRE4-OX plant and JRE4-EAR hairy root lines. Metabolite levels were analyzed by LC-QTOF-MS for α-tomatine and by GC-MS for others. The error bars represent SD from four (for a) or five (for b) biological replicates. Levels of other SGAs are available in Supplementary Table S6. (a) Levels in leaves from JRE4-OX plants (line OX1) exposed to MeJA vapor for 4 d. (b) Levels in hairy roots of JRE4-EAR (line #1) treated with MeJA for 4 d. (c) Metabolites are schematically indicated in SGA biosynthesis pathway.

209x163mm (300 x 300 DPI)

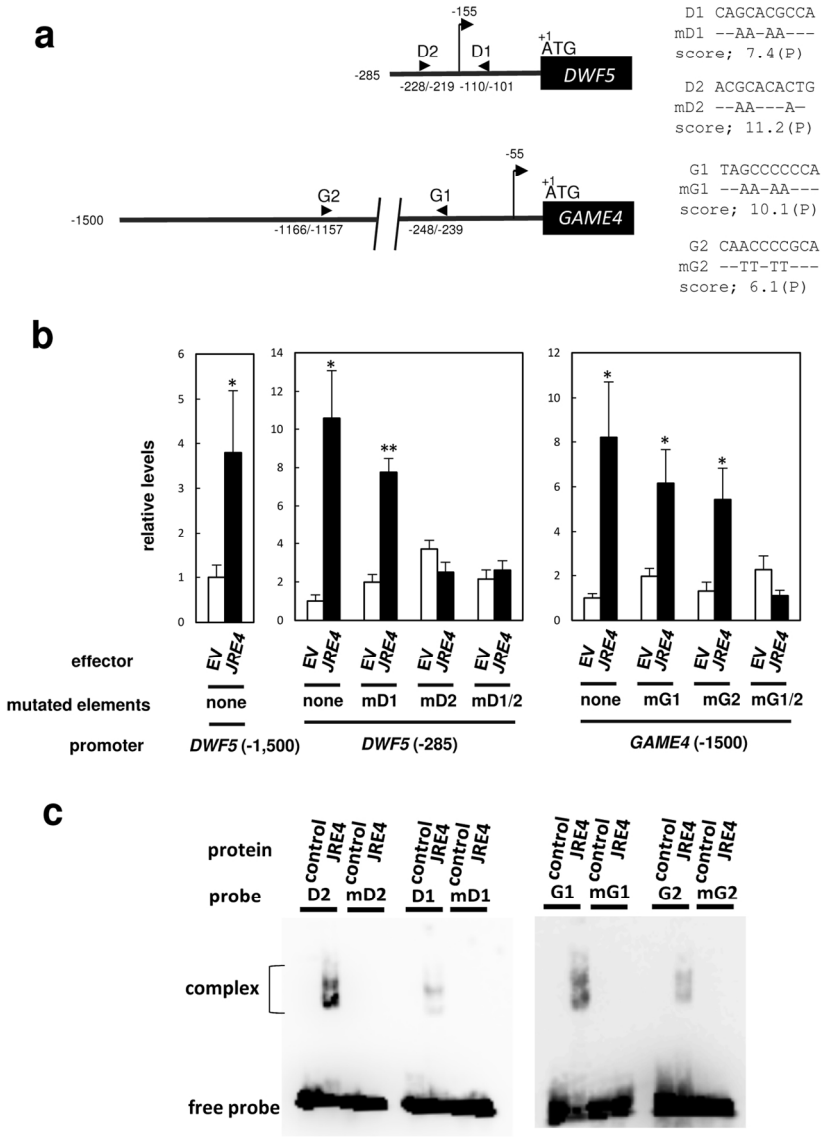


Figure 6 JRE4-mediated activation of DWF5 and GAME4 is dependent on JRE-binding elements found in the promoter regions.

(a) Schematic representation of 5′-flanking regions of DWF5 and GAME4. The positions of JRE-binding elements (arrowheads) and transcriptional start sites (arrows with vertical lines) are shown. On the right, nucleotide sequences of the elements are shown, while only the substituted nucleotides are indicated in mutated versions. (b) Transient transactivation assays in tomato fruits. GUS reporter gene fused with 5′-flanking regions of DWF5 (-1,500 to -1 or -285 to -1; counted from the first ATG) and GAME4 (-1,500 to -1) or their mutated versions, were delivered into tomato fruits by agroinjection with JRE4 effector plasmid or empty vector (EV) and GFP reference plasmid. Expression levels of GUS reporter gene were normalized to those of the GFP reference gene, and are shown as relative values against the values of each wild-type reporter with EV. The bars indicate SD from four independent experiments. Significant differences between EV and JRE4 effector for each reporter were determined by Student's t-test: *P<0.05; **P<0.01. (c) EMSA assay showing in vitro binding of recombinant JRE4 to the predicted elements. Probes were incubated with

proteins from empty vector control or recombinant JRE4. Probe sequences are available in Supplementary Table S10.

119x173mm (300 x 300 DPI)

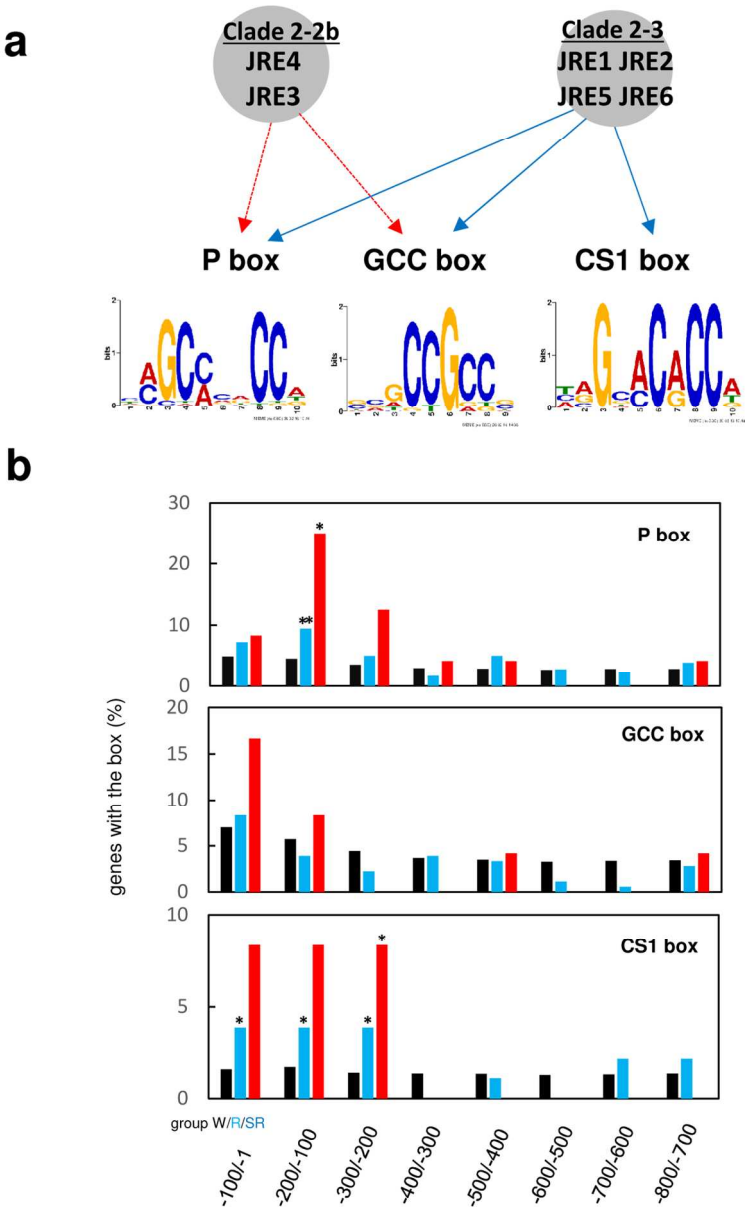


Figure 7 Computational prediction of putative JRE-binding elements in promoter regions of genes regulated by JREs.

(a) Presumed binding elements of JREs. DNA-binding specificities of JRE4 and related ERFs from other species had been studies （Shoji et al. 2013）; the binding of JRE4 to P and GCC boxes was experimentally validated, while those for other JREs are presumed based on the results of clade 2-2b JRE4 for JRE3 and those of clade 2-3 ORCA3 from C. roseus for the remaining four JREs. Sequence logos representing P , CS1 , and GCC boxes were generated by WebLogo (Crooks et al. 2004) based on position-specific probability matrices (Supplementary Table S7), which were determined using the sequences predicted in the 5'-flanking regions (-300 to -1) of group R genes. (b) Genes predicted with JRE-binding elements (scores > 7.0) for indicated region in group W (black), R (blue) and SR (red). The genes of group R (180 JRE-regulated genes) and of group SR (JRE-regulated 24 SGA biosynthesis genes) are given in Supplementary Table S4 and Fig. 3, respectively. Significant differences of values (shown in %) from those for group W (all 34,725 protein-coding genes in tomato genome) were determined by one-sided Fisher's exact test; *P<0.05,

**P<0.01.

119x189mm (300 x 300 DPI)